

# Accumulation by avalanches as significant contributor to the mass balance of a High Arctic mountain glacier

Bernhard Hynek<sup>1,2,3</sup>, Daniel Binder<sup>4,3</sup>, Michele Citterio<sup>5</sup>, Signe Hillerup Larsen<sup>5</sup>, Jakob Abermann<sup>2,3</sup>, Geert Verhoeven<sup>6</sup>, Elke Ludewig<sup>7</sup>, Wolfgang Schöner<sup>2,3</sup>

<sup>1</sup> Geosphere Austria, Department Climate Impact Research, Vienna, Austria

<sup>2</sup> Institut für Geographie und Raumforschung, Universität Graz, Austria

<sup>3</sup> Austrian Polar Research Institute, Vienna, Austria

<sup>4</sup> Institute for Geosciences University of Potsdam, Germany

<sup>5</sup> Geological Survey of Denmark and Greenland, Copenhagen, Denmark

<sup>6</sup> Department of Prehistoric and Historical Archaeology, Universität Wien, Austria

<sup>7</sup> Geosphere Austria, Sonnblick Observatory, Rauris, Austria

Correspondence to: B. Hynek ([bernhard.hynek@geosphere.at](mailto:bernhard.hynek@geosphere.at))

Keywords: UAV; structure from motion photogrammetry; Greenland; glacier mass balance; snow avalanches

## Abstract.

Greenland's peripheral glaciers are losing mass at an accelerated rate and are contributing significantly to sea-level rise, but only a few direct observations are available. Here In this study, we use the unique combination of high-resolution remote sensing data and direct mass balance observations to separate and quantify the contribution of a singular avalanche event to the mass balance of Freya Glacier (74.38° N, 20.82° W), a small (5.5 km<sup>2</sup>, 2021) mountain glacier in Northeast Greenland. Elevation changes calculated from repeated photogrammetric surveys on 11<sup>th</sup>–18<sup>th</sup> in August 2013 and on 28<sup>th</sup>–31<sup>st</sup> July 2021 range from -11 m to 18 m, with a glacier-wide mean of  $1.56 \pm 0.10$  m ( $1.33 \pm 0.21$  m w.e.). Somewhat surprisingly, the The geodetic mass balance over the full entire period of eight years period (2013/14 - 2020/21) is found to be positive, ( $-0.73 \pm 0.22$  m w.e.). A main imprint/significant influence of on the near decadal mass balance stems from the exceptional (2.5 standard deviations above average) winter mass balance of 2017/18, which was 2.5 standard deviations above average with ( $1.85 \pm 0.05$  m w.e.). After heavy snowfall in mid-February 2018, when in addition to above average precipitation, snow avalanches from the surrounding slopes affected more than one third of the glacier surface and contributed  $0.35 \pm 0.05$  m w.e., which is close to 20% to the total winter mass balance of 2017/18. While snow of the 2018 avalanches has still been visible on the glacier surface in summer 2021, we observed also avalanche depositions between 2012 and 2016, but to a much lesser extent. Due to a gap in valid mass balance point observations caused by high accumulation rates and the COVID-19 pandemic the recently reported glacier-wide annual mass balance are rather crude estimates and show a negative bias of -0.22 m w.e. a<sup>-1</sup> in respect compared to the geodetic mass balance, which demands a thorough reanalysis of the glaciological time series. Finally, we speculate that the projected future warming may increases the likelihood of extreme snowfall events for individual years and, thus potentially increasing the contribution of snow avalanches to the mass balance of mountain glaciers in NE Greenland might increase.

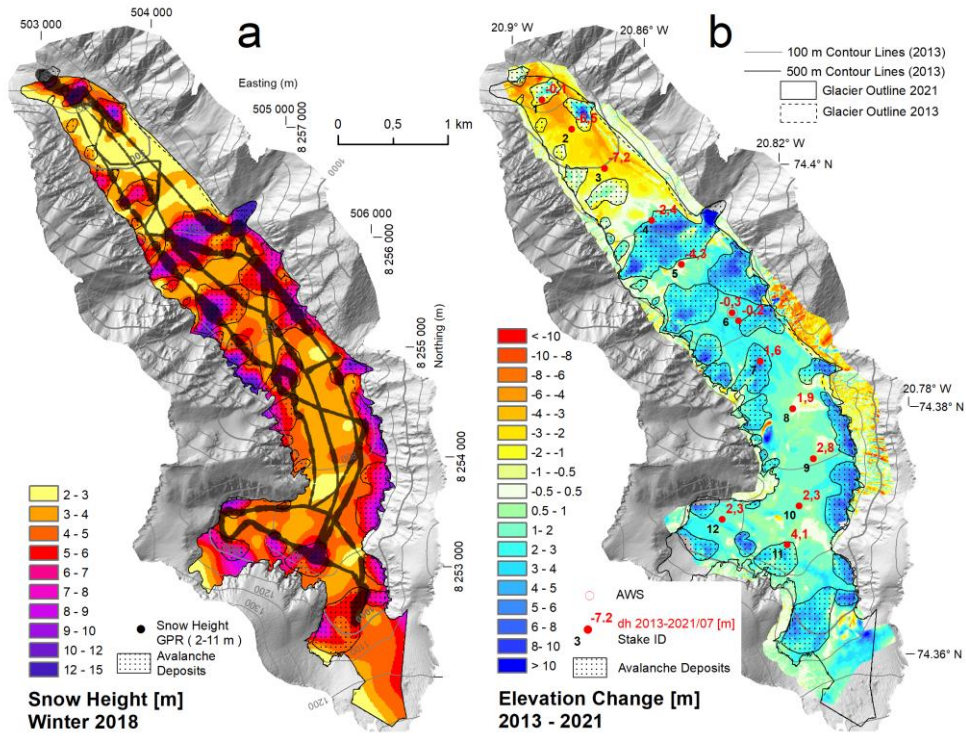
Formatiert: Hervorheben

Formatiert: Hervorheben

Formatiert: Nicht Hervorheben

Formatiert: Hervorheben

Graphical Abstract.



40

a) Measured (GPR) and extrapolated snow height in winter 2018 and ~~delineation~~ delineation of avalanche affected areas. b) Elevation Change between 18.8.2013 and 27.7.2021 and measured ablation at the stake locations.

## 1 Introduction

45 The ice cover of Greenland consists of the Greenland Ice Sheet and approximately ~20 300 peripheral glaciers (Abermann et al., 2019b; Rastner et al., 2012). Although Greenland's peripheral glaciers comprise only 4% of the total ice cover of Greenland, their recent contribution to mass loss from Greenland and global sea-level rise is disproportionately high (11%) in-comparisoned to that of the ice sheet (Khan et al., 2022). This, confirming-confirms their higher sensitivity to ~~the~~ current climate change. During the last 60 years mass loss from Greenland's peripheral glaciers comprise ~ 8% of the world's land ice contribution to  
50 sea-level rise (Frederikse et al., 2020; Zemp et al., 2019).

While the overall mass loss from Greenland's peripheral glaciers has accelerated during the last two decades, the pattern is heterogeneous on a regional scale ~~the pattern is heterogenous~~ (Hugonnet et al., 2021). In Northeast Greenland, particularlyspecifically, the mass loss has decelerated, with continued thinning in-at lower elevations and thickening in-at higher elevations (Khan et al., 2022). The decelerated mass loss in Northeast Greenland has been associated with an increase in precipitation (Hugonnet et al., 2021), whereas the ~~decelerated-reduced~~ mass loss of Icelandic and Scandinavian glaciers, for example, has been associated with North Atlantic Cooling-cooling (Noël et al., 2022).

However, our knowledge of the individual drivers of mass changes of Greenland's peripheral glaciers is limited as direct observations and process studies are scarce. Machguth et al. (2016b) compiled all reported mass balance observations in Greenland and showed that while mass balance observations onat the ice sheet have increased tenfold, the peripheral glaciers are still heavily undersampled despite their topographical and climatological complexity. To our knowledge, currently only 6 out of 20 300 glaciers and icecaps in Greenland are monitored (Abermann et al., 2019b). Three of ~~them-these~~ are located on the 2600 km long east coast: Mittivakkat Glacier on Ammassalik Island (65° N) (Mernild et al., 2013; Yde et al., 2014), A. P. Olsen Ice Cap (Citterio and Ahlstrøm, (2010); Larsen et al., (2023) and Freya Glacier (both at 74° N near Zackenberg Research Station).  
65

The mass balance monitoring at Freya glacier has been carried out using the direct or glaciological method (Kaser et al., 2003; Østrem and Brugmann, 1991) which is based on various point observations of ablation and accumulation distributed over different elevations on the glacier. These point observations of mass change are then extrapolated to estimate the annual mass balance of the whole-entire glacier, often using-incorporating additional information like-such as the position of the snowline. However, the specific implementation of this step may vary among glaciers and observers (Zemp et al., 2013) and also depends also on the number and distribution of available point measurements. Annual mass balance measurements are likely to accumulate systematic errors over the years (e.g. Huss et al., 2009), therefore it is recommended to compare and, if necessary, homogenise the annual mass balance time series using decadal volume changes based on geodetic surveys of the glacier surface (Huss et al., 2009; Klug et al., 2018; Zemp et al., 2013). On Freya Glacier these geodetic surveys were carried out in 2013 and 2021 using an Image-Based 3D surface Modelling (IBM) approach.  
70  
75

In the last decade, IBM-via hybrid photogrammetric computer vision-based approaches haves become commonplace in many academic fields. With photogrammetric methods at their core, these hybrid approaches mainly rely on the computer vision algorithms Structure from Motion (SfM) and Multi-View Stereo (MVS) to digitally extract three-dimensional (3D) surfaces from overlapping images. These 3D surfaces can then be used to produce accurate orthophotographs. Often, such SfM-MVS approaches rely-uponutilize terrestrial photographs acquired with consumer-grade cameras (Piermattei et al., 2015; Marcer et  
80

Formatiert: Englisch (Vereinigte Staaten)

al., 2017) or ~~photos-images~~ obtained via cameras mounted on uncrewed aerial vehicles (UAVs) (e. g. Gindraux et al., 2017; Rossini et al., 2018; Geissler et al., 2021).

Interestingly, there are only a few studies on the contribution of snow avalanches to the mass balance of glaciers ~~although the importance of this accumulation process seems obvious despite the apparent importance of this accumulation process~~. Glaciers with considerable accumulation from avalanches ~~are usually have been~~ associated with high and steep headwalls typical for High Mountain Asia (Laha et al., 2017). ~~(Kneib et al., 2024b) showed, that a lot of glaciers in the European Alps are also avalanche fed. In the Arctic, rising temperatures may increase the number and intensity of snowfall events as observed over NE Greenland in 2018 (e.g. Schmidt et al., 2019) which will in turn enhance avalanche activity (e.g. Abermann et al., 2019a). (Kneib et al., 2024a) However, (The influence-contribution of avalanches on-to the mass balance of individual some Himalayan glaciers is difficult to measure, therefore it has has been quantified by Laha et al. (2017) by applying precipitation factors locally at the base of headwalls to fit the observed ice flux (Laha et al., 2017; (Kneib et al., 2024a; Laha et al., 2017). - but to our knowledge snow avalanches have not been shown to have a significant influence on the mass balance of glaciers outside the Himalaya. With increasing temperatures in the Arctic, precipitation is expected to rise, which may lead to heavier single precipitation events as observed over NE Greenland in 2018 (e.g. Schmidt et al., 2019) which can lead to strong avalanche activity (Abermann et al., 2019a).~~

Formatiert: Hervorheben

This study examines the effects of an extraordinary winter accumulation combined with widespread avalanche activity on the mass balance of an High Arctic mountain glacier. In particular, we quantify the contribution of avalanches to the winter mass balance 2017/18 of Freya Glacier by taking advantage of a detailed ground penetration radar survey of snow depth ~~conducted~~ in April 2018, ~~and we further~~ ~~Furthermore~~ we demonstrate the imprint of avalanches in high-resolution glacier elevation changes 2013 - 2021.

~~In the following we~~ We calculate IBM-derived elevation changes and deduce the geodetic mass balance of Freya Glacier between 2013/14 and 2020/21. We delineate snow avalanche deposits ~~of from~~ February 2018 on the glacier area, ~~and~~ quantify their mass contribution to the winter mass balance 2017/18 and show their imprint on the multi-year geodetic mass balance. Finally, we compare the geodetic mass balance to the cumulative glaciological mass balance, discuss ~~reasons-likely error sources~~ for the ~~differences-discrepancy~~ and ~~stress-emphasise~~ the need for a reanalysis of the glaciological record. ~~This need arises due to the, which suffers from~~ observational gaps caused by travel restrictions during the ~~Covid~~ COVID-19 pandemic and a limited observational network that ~~turned-out proved insufficient-to-be-not-dense-enough-to~~ account for the recent spatial variability of surface mass balance on the glacier.

## 2 Freya Glacier

Freya (~~Freja, Fröya~~) Glacier (74,38° N, 20.82° W) is a polythermal mountain glacier (Binder et al., 2009) ~~situated located~~ on Clavering Island in Northeast Greenland, 10 km southeast of Zackenberg Research Station (Fig. 1). The coastal glacier is oriented towards the Northwest, surrounded by steep ridges on both sides, spans an elevation of 1300 m to 280 m a.s.l. and covers a surface area of 5.5 km<sup>2</sup> (2021). The glacier was subject to glaciological investigations already in the late 1930s (Ahlmann, 1942, 1946) likely due to its ~~rather-relatively~~ good accessibility. During the International Polar Year 2007/2008 a mass balance monitoring programme was initiated (Schöner et al., 2009) ~~which-and~~ has been ongoing since. ~~(Hynek et al., 2014; World Glacier Monitoring Service (WGMS), 2023).~~ The current monitoring consists of a stake network, an automatic weather station (AWS) of the PROMICE setup (Fausto et al., 2021) and two high-quality webcams (Hynek et al., 2018). Daily

Kommentiert [HB1]: Origin of different spellings in Fußnote erklären.

125

images ~~from the~~ two webcams are publicly available via the websites foto-webcam.eu (~~Freya Glacier Webcam 1: <https://www.foto-webcam.eu/webcam/freya1/> and Freya Glacier Webcam 2: <https://www.foto-webcam.eu/webcam/freya2/>~~). (~~Freya Glacier Webcam 1, 2023; Freya Glacier Webcam 2, 2023~~).

### 3 Data and Methods

#### 3.1 Geodetic Survey 2013

130 Due to the ease of the process and the suitable topography, SfM-MVS-based image-based 3D surface modelling was the optimal  
choice for generating a DEM of Freya Glacier during the 2013 field campaign. ~~Although no~~ UAV was available, ~~but~~ the  
ridges around the glacier ~~offered~~ provided useful natural viewpoints for a ground-based survey. Between 11<sup>th</sup> and 18<sup>th</sup> August  
2013, we took oblique overlapping photographs of the glacier surface from about 450 locations on the slopes on both sides of  
135 the glacier using a Nikon D7100 digital single lens reflex camera with a 20 mm fixed lens. Simultaneously with the image  
acquisition, we surveyed ~~approximately~~ ~100 natural Ground Control Points (GCPs) using a differential GNSS (Global  
Navigation Satellite System) receiver (Fig. 2 a-c). For post-processing of the survey, a temporary GNSS reference station was  
established on stable rock next to the glacier. We surveyed the upper part of the glacier on the 11<sup>th</sup> and 12<sup>th</sup> of August 2013,  
when the glacier surface was almost snow-free. Snowfall ~~event~~ on 14<sup>th</sup> August followed by a period of low visibility marked  
140 the end of the melt season. On 18<sup>th</sup> August 2013, we surveyed the lower part of the glacier. Surface ablation between the survey  
dates was below 0.15 m and was partly compensated by an average fresh snow height of 0.10 m.

#### 3.2 Geodetic Survey 2021

The second high-resolution DEM used in this study stems from 2021. On 29<sup>th</sup> and 31<sup>st</sup> July 2021, we used a UAV (DJI Phantom  
4 RTK) to obtain an overlapping image series of the glacier surface. On 29<sup>th</sup> July, we photographed 80% of the glacier surface  
145 (lower part) and finished the drone flights on 31<sup>st</sup> of July. On 28<sup>th</sup> and 29<sup>th</sup> of July 2021, we surveyed ~~approximately~~ ~100  
mainly artificial GCPs on the glacier surface using a differential GNSS receiver and a base station that was put up at the same  
location as in 2013 (Fig. 2 d-f). During the survey, surface ablation between 28<sup>th</sup> and 31<sup>st</sup> July was less than 0.2 m. Table 1  
lists the main characteristics of both photogrammetric surveys.

#### 3.3 GNSS and IBM workflow

GNSS raw logs containing the GCPs and the UAV trajectory were post-processed using the reference station next to the glacier.  
150 Coordinates were transformed into UTM coordinate reference system (zone 27N, epsg:32627) and to orthometric heights  
(egm96). For the accuracy assessment of the surface reconstruction, one subset of the GCPs was used to reference the generated  
3D model (control points), and another subset was used to validate the 3D model (independent check points). All GCPs were  
used to reference the final DEM. GCPs that were not clearly visible in the imagery were used for elevation validation of the  
final DEM output. The workflow of the DEM and orthophoto generation followed the classical SfM process (e.g. Rossini et al.,  
155 2018) using Agisoft Metashape (AgiSoft LLC, 2023). Due to the different surface texture (snow covered vs snow free) of the  
lower and upper 2013 imagery, these parts of the glaciers were processed independently and combined to one final DEM  
afterwards (see supplement).

#### 3.4 Elevation Changes

Elevation ~~c~~Changes ~~between~~ 2013 ~~and~~ 2021 were calculated by DEM differencing in 1 m planar resolution. ~~As the~~  
160 ~~g~~Georeferencing of the two final DEMs is based on ~~all a large number of~~ ~~respective~~ GCPs, a co-registration of the DEMs (Nuth  
and Kääb, 2011) was not ~~carried out~~ necessary. ~~Elevation differences in overlapping ice-free terrain had a mean bias of 0.1 m~~  
~~and a standard error of 0.45 m (see supplement). Most of the likely stable terrain is rather steep, and in some areas the DEM~~  
~~2013 might have larger errors than everywhere else, so we did not correct for this bias, as the overlapping area on stable terrain~~  
~~outside the glacier is too small. However the small overlapping and supposed stable area was used to calculate error statistics~~  
165 ~~of the two DEMs (see supplement).~~

Formatiert: Nicht Hervorheben

Formatiert: Nicht Hervorheben

### 3.5 Density Assumption and Geodetic Mass Balance

To convert the observed volume change into a mass change we use the conversion factor of  $850 \pm 60 \text{ kg/m}^3$  recommended by Huss ~~et al.~~ (2013) for periods longer than 5 years, ~~with~~ stable mass balance gradients, the presence of a firn area and volume changes significantly different from zero. No firn density measurements have been carried out on the glacier so far, neither in the accumulation zone nor in one of the avalanche deposits. The main part of the accumulation that led to the observed positive elevation changes ~~had happened/occurred already~~ in 2018 and has ~~experienced/undergone~~ densification ~~over~~ ~~in~~ ~~4~~ ~~four~~ melt seasons ~~at the date by the time~~ of the second survey. However, percolation and the possible formation of ice lenses might create a high variability in firn density (Vandecrux et al., 2018, Machguth et al., 2016a). ~~Therefore, so~~ we decided to follow the recommendation of Huss ~~et al.~~ (2013). In 2013 the survey was very close to the end of the ablation season, ~~in~~ in 2021 an adjustment of  $-0.6 \pm 0.05 \text{ m w.e.}$  ~~was calculated~~ between the survey on 29<sup>th</sup> July and the end of the ablation season on 5<sup>th</sup> September ~~was calculated~~ based on 10 ablation stake readings.

### 3.6 Glaciological mass balance

#### 3.6.1 Winter mass balance

Due to logistical challenges in accessing the glacier with a snow mobile, the number of snow height observations varies considerably from year to year. Distributed winter snow height is measured either by 40 - 150 manual snow depth probings, or by a 800 MHz GPR snow survey of several km in length. In April 2018, an extended GPR snow survey with a total length of 27 km was carried out to ~~get a good picture of/capture~~ the spatial distribution of snow depth including the still visible avalanche deposits. To get a regular grid of snow height, a spline function was fitted to the data. In contrast, snow density was measured at only one location, which was not influenced by avalanches: in a snow pit next to the AWS at an elevation of 680 m (Fig. S4). ~~Winter mass balance was calculated as a spatial average of snow depth over the whole glacier area multiplied with the measured snow density next to the AWS.~~ GPR snow surveys of a similar point observation density have been carried out in spring 2008 and 2017.

#### 3.6.2 Annual mass balance

Until 2015 annual mass balance measurements were usually carried out in August, and ~~ablation and accumulation/seasonal mass balance~~ was measured at several points distributed ~~over/across~~ the glacier. Annual glacierwide mass balance was then determined by ~~extrapolating~~ the point values onto the whole glacier area. Depending on the number of point observations the mean standard error is estimated as  $0.05 \text{ m w.e. a}^{-1}$ . Mainly due to high travel costs, but also in accordance with the mass balance monitoring at A. P. Olsen Ice Cap the monitoring strategy was changed in 2016 to only one visit per year in spring, ~~and a~~ ~~At~~ the same time an automatic monitoring system was installed, namely an automatic weather and mass balance station and an automatic camera to ~~follow-track~~ the retreat of the snow line during summer. Since then annual mass balance ~~has~~ still ~~been~~ measured at eleven ablation stakes, which usually ~~stick out of/protrude from~~ the winter snow. At ~~each~~ stake the mass balance of the previous year is determined by measuring the ~~actual-current~~ snow depth and the height change of the stake. However, because of above average snow heights in spring 2018 and 2019 only two stakes were found. In 2020 and 2021 spring measurements were not possible due to the travel restrictions caused by the COVID-19 pandemic. Therefore, the glacier-wide

mass balance from 2016/2017 to 2020/21 was reconstructed using a linear relationship (see supplement for details) between the mass balance at the AWS (index stake) and the glacier-wide mass balance based on observations from 2008 to 2016, introducing an estimated uncertainty of 0.2 m w.e. a<sup>-1</sup>. ~~In July 2021 and in spring 2022, most~~ Most stakes were found again and could be measured ~~in July 2021 and April 2022.~~

### 3.7 Quantifying the influence of avalanches on the winter mass balance of 2018

To delineate the avalanche deposits of 2018 we ~~used a strong increase~~ identified areas with a strong increase of snow heights along the GPR tracks. ~~To complete the delineation in~~ In areas without GPR tracks, we ~~completed the delineation used using~~ a best estimate based on ~~fotos-pictures~~ photos of avalanche cracks, remnants of avalanches in the ortho~~ph~~photo of 2021, ~~and~~ above average local elevation changes 2013-2021 ~~together with~~ and likely avalanche flow paths based on topography. The GPR snow depth data ~~set~~ was sampled down to 10 m point distance and then interpolated using a spline function onto a grid of glacier-wide snow heights. To estimate the contribution by avalanches to the winter mass balance of 2018, we calculated spatial averages of the snow height grid ~~on-in~~ avalanche affected areas and ~~on-in~~ avalanche free areas. To ~~transfer-convert~~ snow heights into snow water equivalent, we used the mean snow density of 385 kg m<sup>-3</sup> (measured in the snow pit next to the automatic weather station) for areas without avalanche deposits, and a 5% ~~to~~ (10%) increased snow density ~~for~~ in avalanche areas, as snow density ~~usually typically~~ increases with snow depth and avalanche deposits have higher snow densities ~~than~~ as the undisturbed snow pack ~~well~~.

### 3.8 Climate data

Snow height at the AWS on Freya Glacier is measured by two Campbell SR 50 ultrasonic devices, one fixed ~~to~~ at the mast of the weather station 3.4 m above the ground and one fixed ~~to~~ at an ablation stake. Both sensors were ~~snowed-in~~ buried in snow ~~by in mid-February~~ mid-February 2018. On 28<sup>th</sup> April, the weather station was reestablished on the surface (Fig. 5). The data gap of 2.5 months was reconstructed using snow height data from the main weather station at A. P. Olsen Ice Ceap (Larsen et al., 2023; Greenland Ecosystem Monitoring, 2020a), which has a continuous record in 2018. ~~Further-Additionally~~, we used temperature data from the climate station Zackenberg (Greenland Ecosystem Monitoring, 2020b) and precipitation data from the ERA5 global reanalysis (Hersbach et al., 2020).

Feldfunktion geändert

Formatiert: Englisch (Vereinigte Staaten)

Formatiert: Englisch (Vereinigte Staaten)



## 4. Results

Formatiert: Englisch (Vereinigte Staaten)

### 4.1 DEM and orthophoto 2013

The shaded relief of the 2013 DEM (Fig. 3a) shows a high level of detail, ~~with~~ Only a few artefacts ~~are~~ visible in the middle ~~part of the glacier~~ and ~~in the~~ uppermost part ~~of the glacier~~. ~~These artefacts occur~~, where the distance ~~of between~~ the photo points ~~to and~~ the glacier surface is high and the angle ~~to~~ towards the glacier surface is acute. ~~Especially the~~ ~~The~~ middle part of the glacier is poorly covered, the GCPs there (Fig 3a, set 3) could not be identified in the images and were used to check only the vertical accuracy of the DEM in that area (Table 2). The ortho~~ph~~photo shows almost snow-free conditions in the upper part of the glacier and the new snow on the lower part ~~of the glacier~~ (Fig. 3b). The surface reconstruction covers the ~~whole entire~~ glacier area and the adjacent ridges. ~~Since~~ ~~As~~ all GCPs are on the glacier surface, the accuracy of the surface reconstruction is expected to drop significantly in the adjacent ridges. The accuracy of the surface reconstruction expressed as RMSE at the check points is significantly worse than the RMSE at the control points, ~~where with especially the~~ lateral accuracy ~~being particularly poorer is worse~~ than the vertical accuracy (Table 2).

Formatiert: Englisch (Vereinigte Staaten)

### 4.2 DEM and orthophoto 2021

The shaded relief of the 2021 DEM (Fig. 4a) shows a much higher level of detail due ~~to the~~ better measurement geometry and resolution. The ground sample density (Table 1) and the accuracy of the surface reconstruction (Table 2) of the 2021 survey are both higher ~~thathann~~ ~~those~~ for the 2013 survey. However, only 95% of the glacier surface is reconstructed, and the DEM does not extend much to the adjacent ridges ~~due to limited~~, as UAV battery supply ~~was limited~~ during ~~the~~ fieldwork. ~~Remnants of the 2018 avalanche deposits~~ ~~Avalanche affected areas~~ are still visible in the orthophoto (Fig. 4b) on the lower and middle part of the glacier, while the upper part was still covered by slush and winter snow.

### 4.3 Elevation Changes and Geodetic Mass Balance

Elevation changes in 1 m resolution (Fig. 5b) were calculated for 95% of the glacier area, missing only some smaller parts in the upper accumulation zone. Elevation changes for these areas were calculated by fitting a spline function to the elevation changes in the surrounding ~~areass~~, to avoid a bias in the geodetic mass balance. Elevation changes show a high spatial variability. Surface lowering is observed on 20% of the glacier surface, mainly at elevations below 600 m a.s.l., and reaching a minimum of -11 m in the lowest part of the glacier. Above 600 m a.s.l. elevation changes are mainly positive. At the centerline of the glacier, elevation gains are mainly smaller than 2 m. In several distinct areas predominantly along both sides of the glacier, elevation gains are up to several meters with a maximum of 17 m. These areas coincide with potential avalanche depositions from large side valleys. The mean elevation change ~~08/ from August 2013 to- July 07/2021~~ for the entire glacier is  $1.56 \pm 0.10$  m. ~~The m~~ ~~Main sources of uncertainty is introduced by~~ ~~include~~ ablation during the survey, unmeasured areas, and the uncertainty in the delineation of the glacier surface area. -Converting this volume change into a mass change – and hereby introducing another uncertainty using a density assumption of  $850 \pm 60$  kg/m<sup>3</sup> – we obtain the specific geodetic mass balance ~~from August 2013 to July 2021~~ ~~08/2013 – 07/2021~~ as  $b_{\text{geod}} = 1.33 \pm 0.21$  m w.e. After accounting for the mass losses during August 2021, the total 8-year geodetic mass balance 2013/14 - 2020/21 is adds up to:  $b_{\text{geod.8y}} = 0.73 \pm 0.22$  m w.e.

Formatiert: Nicht unterstrichen

### 4.4 ~~The 2018 avalanche eye~~ ~~Winter 2018 and avalanches~~

In ~~the~~ winter ~~of~~ 2017/2018, a series of low pressure systems between the southern tip of Greenland and Iceland transported humidity to the East Coast of Greenland, ~~resulting and resulted~~ in above average snowfall ~~along the entire on the whole~~ East Coast (Fig. 8). Between 12<sup>th</sup> and 18<sup>th</sup> ~~February 2018 accumulated –approximately 1.5 m of snow accumulated within five~~ 5

Formatiert: Hochgestellt

Formatiert: Hochgestellt

270 days on Freya Glacier. This led to widespread avalanche activity, ~~and onto the glacier surface, so that~~ during fieldwork in April 2018, signs of large avalanche deposits were visible ~~all over~~ across the ~~entire~~ glacier. ~~Especially~~ ~~Particularly~~ in the middle part of the glacier, several large avalanches originating from the tributary valleys on both sides ~~of the glacier~~ covered large parts of the glacier. In April 2018, avalanche deposits were found on 36% of the glacier area. Individual GPR-derived snow heights ranged from 2.2 m up to 12.1 m, with a median snow height of 4.0 m. The distribution of snow height and the delineation of avalanche ~~influenced-affected~~ areas ~~is-are~~ shown in Fig. 6a. ~~The a-~~Area-averaged ~~value of snows~~ snow height on the entire glacier is 4.8 m, ~~with 6.2 m on~~ ~~on~~ avalanche deposits ~~-6.2 m~~, and ~~4.0 m in~~ ~~in~~ areas ~~without no~~ ~~no~~ avalanches, ~~-4.0 m~~. The snow height contribution from avalanches averaged over the whole glacier is 0.8 m. Mean snow density at the snow pit next to the AWS at stake 6 was 385 kg/m<sup>3</sup>. Assuming ~~thise same-bulk~~ snow density everywhere on the glacier, the specific mass balance contribution of avalanches is 0.31 m w.e., which ~~accounts foris~~ 17% of the total winter mass balance of 1.85 ± 0.05 m w.e. ~~This can be seen-We consider this~~ as a lower limit as ~~the~~ avalanche snow likely has a higher ~~snow~~ density than the undisturbed ~~snoweoversnow cover~~ in the middle of the glacier (Sovilla et al., 2001), where the snow density measurement was carried out (Sovilla et al., 2001). If we assume an increase in ~~bulk~~ snow density of 5% (10%) % due to compaction and overburden pressure within the avalanche deposits, the mass contribution of avalanches would be 0.35 (0.39) m w.e., ~~being-representing~~ 18 (20)% of ~~thea~~ winter mass balance of 1.89 (1.93) m w.e. Remnants of the avalanches are still visible on the glacier surface 3 years after the incident (Fig. 4b, Fig. 7c,e, Fig 11) and have altered local surface mass balance significantly at stake 1, 4 and 11 compared to the surrounding stakes (see stake readings in Fig 6b and Table S1).

#### 4.5 Imprint of avalanches on the elevation changes

290 While remnants of small snow avalanches ~~are-have been~~ visible on the glacier surface ~~overin~~ several years, ~~especially~~ ~~particularly~~ between 2012 and 2016 (Fig. 10, Fig.11), their surface extent is rather limited. At least five avalanche deposits are visible on the orographic right side of the glacier ~~on-in~~ orthophotos ~~taken~~ in July and August 2016 (Fig. 10) and to a lesser extent also ~~in~~ the orthophoto ~~of-from~~ 2012.

#### 4.7 Glaciological mass balance 2013/14- 2020/21

295 The ~~timeseries~~ time series of winter and annual mass balances (World Glacier Monitoring Service, 2022) of Freya Glacier are shown in Fig. 11. Prior to the first DEM in 2013, mass balances were more negative, ~~especially-the mass-balance-of-with~~ 2013 ~~was-so-far-thehaving the~~ most negative mass balance on record. Especially stake 1 and stake 4 are influenced by avalanches and show reduced ablation rates. The cumulative glaciological mass balance 2013/14 - 2020/21 is -1.0 + 0.4 m w.e. The bias with respect to the geodetic mass balance is -1.73 m w.e. or -0.22 m w.e. a<sup>-1</sup>.

### 300 5 Discussion

A major uncertainty in the geodetic mass balance is introduced by the density assumption. Measurements of firn density in Greenland (Braithwaite et al., 1994; Vandecrux et al., 2018) have shown; that the firn density varies a lot depending on the amount of accumulation and melt at a specific site, ~~and~~ particularly ~~on-due to~~ the formation of ice layers by percolating meltwater. Machguth et al. (2016a) showed; that firn loses a part of its capacity to store water after ~~building-forming near-~~ surface ice layers during strong melt events. Huss (2013) ~~has showedn~~ in a model experiment; that a conversion factor between elevation change and mass change of 850 ± 60 kg m<sup>-3</sup> is appropriate for a wide range of conditions over longer time periods,

310 but that this factor can vary significantly on timescales ~~below~~shorter than 10 years. On Freya Glacier, high accumulation rates by avalanches have generated thick and possibly dense firn layers with high potential of meltwater retention and refreezing. However, it is difficult to constrain the snow density of the avalanche snow without a direct measurement. Li et al. (2021) and Sovilla et al. (2001) observed that the snow density of avalanche deposits might be two ~~to~~or three times higher than the undisturbed snowpack at the time of the avalanche release date. Refreezing of meltwater has already been suspected to play an important role in the mass balance of Freya Glacier (Ahlmann, 1946) and ~~has been~~was ~~observed~~ qualitatively during fieldwork in 2021. The bright glacier surfaces, that are the remnants of the 2018 avalanches, looked like snow, but proved to be as hard as ice.

315 The cumulative glaciological mass balance for the period 2013/14 – 2020/21 was estimated in a rather crude way and carries uncertainties for several reasons. The accumulation in the avalanche deposits visible in the satellite images ~~from~~of 2014 ~~to~~ 2016 might have been underestimated. ~~In the years~~From 2017 ~~to~~ 2021, only one or two point observations were available, so the glacier-wide mass balance was reconstructed using a linear relationship based on the mass balance at the AWS (stake 6).  
320 Another likely reason for the bias between the glaciological and geodetic mass balance is the internal accumulation by percolation of meltwater and refreezing within deeper layers of the avalanche deposits and in firn generally. This process is ~~generally~~ difficult to measure; in our case it was not feasible to measure firn density due to logistical reasons. A thorough reanalysis of the annual mass balance series using all available data and following a methodology based on Zemp et al. (2013) is intended, but beyond the scope of this paper.

325 Regardless of the recent uncertainty in the glaciological mass balance time series of Freya Glacier there is a shift from rather negative to less negative mass balances with starting in 2013/2014, which we attribute to higher winter accumulation between 2014 and 2018. This shift to less negative mass balances – caused by an increase in precipitation over NE Greenland in recent years – has been shown to be a regional effect by Hugonnet et al. (2021) and Khan et al. (2022).

## 6 Conclusions

Formatiert: Standard

335 Our study shows that the 8-year geodetic mass balance of Freya Glacier from 2013/14 to 2020/21 of Freya Glacier has been positive (0.73 ± 0.22 m w.e.). A significant positive contribution to the mass balance stems from avalanches originating from the surrounding slopes. While avalanche deposits are visible on the glacier surface to a limited extent almost every year to a limited extent, the winter 2018 was clearly was outstanding. After a heavy precipitation event in mid-February 2018, which causing caused a snow height increase of ~1.5 m within 5 days, widespread avalanche activity affected more than one third of the glacier area. Based on a detailed GPR survey conducted in April 2018, we estimated the contribution of avalanches to the winter mass balance of 2018 to be 0.35 ± 0.05 m w.e., which is close to 20%. We showed that avalanche deposits are have, still been visible on the glacier surface three years later, in summer 2021, and leaving a strong imprint on the elevation changes. A main uncertainty in this assessment is introduced arises by from a lack of snow and firn density measurements, particularly especially within the avalanche deposits, but also in the upper firn areas. The cumulative glaciological mass balance for 2013/14 to 2020/21 is negative (-1.0 ± 0.4 m w.e.), it suffers suffering from data gaps and only a few point observations in recent years. The magnitude of the bias between geodetic and glaciological mass balance (-0.22 m w.e. ± 1) is similar to bias estimates reported by (Andreassen et al., (2016) for ten glaciers in Norway and therefore as such not unexpected (see also Zemp et al., 2013). The reason for the large bias of the glaciological record of -0.22 m w.e. ± 1 in regard to the geodetic record needs further investigation using a distributed mass balance model. Likely reasons for this large bias are include the underestimation of the mass contribution by avalanches, the general lack of distributed accumulation measurements in general, and maybe possibly also the underestimation of refreezing meltwater. Capturing these processes, as well as firn density measurements, should receive more attention in future mass balance monitoring at Freya Glacier. Assuming a higher likelihood of strong winter precipitation events in a warmer climate, we expect that accumulation by avalanches might to become more important on Arctic mountain glaciers that are situated in or surrounded by steep terrain.

Formatiert: Schriftart: (Standard) Times New Roman

Formatiert: Schriftart: (Standard) Times New Roman, Nicht unterstrichen

Formatiert: Schriftart: (Standard) Times New Roman

Formatiert: Schriftart: (Standard) Times New Roman

Formatiert: Schriftart: (Standard) Times New Roman, Nicht unterstrichen

Formatiert: Schriftart: (Standard) Times New Roman

Formatiert: Schriftart: (Standard) Times New Roman

Formatiert: Schriftart: (Standard) Times New Roman

Formatiert: Schriftart: (Standard) Times New Roman

Formatiert: Schriftart: (Standard) Times New Roman, Nicht unterstrichen

Formatiert: Schriftart: (Standard) Times New Roman

Formatiert: Schriftart:

Formatiert: Schriftart: (Standard) Times New Roman

Formatiert: Schriftart: (Standard) Times New Roman, Nicht Hochgestellt/ Tiefgestellt

Formatiert: Schriftart:

Formatiert: Schriftart:

Formatiert: Schriftart:

Formatiert: Schriftart: (Standard) Times New Roman

Formatiert: Schriftart: (Standard) Times New Roman, Nicht Hochgestellt/ Tiefgestellt

Formatiert: Schriftart: (Standard) Times New Roman

Formatiert: Schriftart: (Standard) Times New Roman

### Data availability

360 Mass balance data of Freya Glacier are available through the WGMS (wgms.ch) and pangaea.de. The DEMs and orthophotos of 2013 and 2021 have been submitted to pangaea.de. Until the data are Data which are not yet available there, they can be requested from the authors.

### Author Contributions

365 BH designed the study, conducted the data analysis and wrote the manuscript. BH, DB carried out the geodetic surveys. BH, DB, MC, SHL, JA and WS carried out mass balance observations on Freya Glacier. DB analysed the GPR data. GV helped with planning and processing of the 2013 geodetic survey. WS and EL provided the funding. All authors provided insights regarding the interpretation of data and reviewed and edited the manuscript.

370 The authors declare that they have no conflict of interest.

### **Acknowledgements**

The work is supported by the International School for Alpine Research at Sonnblick Observatory (ISAR-SBO), a research Grant from GeoSphere Austria. The survey in 2013 was supported by Österreichische Gesellschaft für Polarforschung. Data from the Greenland Ecosystem Monitoring Programme were provided by the Geological Survey of Denmark and Greenland (GEUS), Denmark and Asiaq – Greenland Survey, Nuuk, Greenland. The authors are grateful to the logistics team at Zackenberg Research Station for the logistical support of the fieldwork. The authors gratefully acknowledge Geo Boffi for post-processing the GNSS data of 2013 and Anders Anker Bjørk for taking overlapping imagery from an airplane in August 2016.

375

## References

380

Abermann, J., Eckerstorfer, M., Malnes, E., and Hansen, B. U.: A large wet snow avalanche cycle in West Greenland quantified using remote sensing and in situ observations, *Nat Hazards*, 97, 517–534, <https://doi.org/10.1007/s11069-019-03655-8>, 2019a.

385

Abermann, J., Van As, D., Wacker, S., Langley, K., Machguth, H., and Fausto, R. S.: Strong contrast in mass and energy balance between a coastal mountain glacier and the Greenland ice sheet, *J. Glaciol.*, 65, 263–269, <https://doi.org/10.1017/jog.2019.4>, 2019b.

AgiSoft LLC (2023):, 2023.

Ahlmann, H. W.: Studies in Northeast Greenland: Part III: Accumulation and Ablation on the Frøya Glacier: Its Regime in 1938-39 and in 1939-40, *Geografiska Annaler*, 24, 1–22, 1942.

390

Ahlmann, H. W.: The Frøya Glacier 1939-40: Accumulation and Ablation on the Frøya Glacier, *Geografiska Annaler*, 28, 239–257, 1946.

Andreassen, L. M., Elvehøy, H., Kjöllmoen, B., and Engeset, R. V.: Reanalysis of long-term series of glaciological and geodetic mass balance for 10 Norwegian glaciers, *The Cryosphere*, 10, 535–552, <https://doi.org/10.5194/tc-10-535-2016>, 2016.

Binder, D., Schöner, W., Brückl, E., Hynek, B., and Weyss, G.: Ground Penetrating Radar Investigations in the North East of Greenland, in: *Geophysical Research Abstracts*, EGU General Assembly 2009, Wien, 2009.

395

Braithwaite, R. J., Laternser, M., and Pfeffer, W. T.: Variations of near-surface firn density in the lower accumulation area of the Greenland ice sheet, Pákitsoq, West Greenland, *J. Glaciol.*, 40, 477–485, <https://doi.org/10.3189/S002214300001234X>, 1994.

400

Citterio, M. and Ahlstrøm, A. P.: The GlacioBasis glacier monitoring programme at A.P. Olsen Ice Cap (Zackenber, NE Greenland), in: *Nordic Glaciology. Abstract from Glaciological Society Nordic Branch Meeting, 28-30 October 2010, Copenhagen, 2010.*

Fausto, R. S., Van As, D., Mankoff, K. D., Vandecrux, B., Citterio, M., Ahlstrøm, A. P., Andersen, S. B., Colgan, W., Karlsson, N. B., Kjeldsen, K. K., Korsgaard, N. J., Larsen, S. H., Nielsen, S., Pedersen, A. Ø., Shields, C. L., Solgaard, A. M., and Box, J. E.: Programme for Monitoring of the Greenland Ice Sheet (PROMICE) automatic weather station data, *Earth Syst. Sci. Data*, 13, 3819–3845, <https://doi.org/10.5194/essd-13-3819-2021>, 2021.

405

Frederikse, T., Landerer, F., Caron, L., Adhikari, S., Parkes, D., Humphrey, V. W., Dangendorf, S., Hogarth, P., Zanna, L., Cheng, L., and Wu, Y.-H.: The causes of sea-level rise since 1900, *Nature*, 584, 393–397, <https://doi.org/10.1038/s41586-020-2591-3>, 2020.

Greenland Ecosystem Monitoring: ClimateBasis Zackenberg - Air temperature - Air temperature, 200cm @ 60min sample (°C) (1.0), <https://doi.org/10.17897/XV96-HC57>, 2020.

410

Hersbach, H., Bell, B., Berrisford, P., Hirahara, S., Horányi, A., Muñoz-Sabater, J., Nicolas, J., Peubey, C., Radu, R., Schepers, D., Simmons, A., Soci, C., Abdalla, S., Abellan, X., Balsamo, G., Bechtold, P., Biavati, G., Bidlot, J., Bonavita, M., De Chiara, G., Dahlgren, P., Dee, D., Diamantakis, M., Dragani, R., Flemming, J., Forbes, R., Fuentes, M., Geer, A., Haimberger, L., Healy, S., Hogan, R. J., Hólm, E., Janisková, M., Keeley, S., Laloyaux, P., Lopez, P., Lupu, C., Radnoti, G., De Rosnay, P., Rozum, I., Vamborg, F., Villaume, S., and Thépaut, J.: The ERA5 global reanalysis, *Quart J Royal Meteor Soc*, 146, 1999–2049, <https://doi.org/10.1002/qj.3803>, 2020.

415

Higgins, A. K.: Exploration history and place names of northern East Greenland, *GEUS Bulletin*, 21, 1–368, <https://doi.org/10.34194/geusb.v21.4735>, 2010.

420

Hugonnet, R., McNabb, R., Berthier, E., Menounos, B., Nuth, C., Girod, L., Farinotti, D., Huss, M., Dussailant, I., Brun, F., and Kääh, A.: Accelerated global glacier mass loss in the early twenty-first century, *Nature*, 592, 726–731, <https://doi.org/10.1038/s41586-021-03436-z>, 2021.

Huss, M.: Density assumptions for converting geodetic glacier volume change to mass change, *The Cryosphere*, 7, 877–887, <https://doi.org/10.5194/tc-7-877-2013>, 2013.

- Huss, M., Bauder, A., and Funk, M.: Homogenization of long-term mass-balance time series, *Ann. Glaciol.*, 50, 198–206, <https://doi.org/10.3189/172756409787769627>, 2009.
- 425 Hynek, B., Weyss, G., Binder, D., Schöner, W., Abermann, J., and Citterio, M.: Mass balance of Freya Glacier, Greenland since 2007/2008, , <https://doi.org/10.1594/PANGAEA.831035>, 2014.
- Hynek, B., Binder, D., and Citterio, M.: The Mass balance of Freya Glacier, Greenland, in 2015/2016. Technical Document, ZAMG, 2018.
- Kaser, G., Fountain, A., and Jansson, P.: A manual for monitoring the mass balance of mountain glaciers, 2003.
- 430 Khan, S. A., Colgan, W., Neumann, T. A., van den Broeke, M. R., Brunt, K. M., Noël, B., Bamber, J. L., Hassan, J., and Björk, A. A.: Accelerating Ice Loss From Peripheral Glaciers in North Greenland, *Geophysical Research Letters*, 49, <https://doi.org/10.1029/2022GL098915>, 2022.
- Klug, C., Bollmann, E., Galos, S. P., Nicholson, L., Prinz, R., Rieg, L., Sailer, R., Stötter, J., and Kaser, G.: Geodetic reanalysis of annual glaciological mass balances (2001–2011) of Hintereisferner, Austria, *The Cryosphere*, 12, 833–849, <https://doi.org/10.5194/tc-12-833-2018>, 2018.
- 435 Kneib, M., Dehecq, A., Gilbert, A., Basset, A., Miles, E. S., Juvet, G., Jourdain, B., Ducasse, E., Beraud, L., Rabatel, A., Mouginot, J., Carcanade, G., Laarman, O., Brun, F., and Six, D.: Distributed surface mass balance of an avalanche-fed glacier, <https://doi.org/10.5194/egusphere-2024-1733>, 2 July 2024a.
- Kneib, M., Dehecq, A., Brun, F., Karbou, F., Charrier, L., Leinss, S., Wagnon, P., and Maussion, F.: Mapping and characterization of avalanches on mountain glaciers with Sentinel-1 satellite imagery, *The Cryosphere*, 18, 2809–2830, <https://doi.org/10.5194/tc-18-2809-2024>, 2024b.
- Laha, S., Kumari, R., Singh, S., Mishra, A., Sharma, T., Banerjee, A., Nainwal, H. C., and Shankar, R.: Evaluating the contribution of avalanching to the mass balance of Himalayan glaciers, *Ann. Glaciol.*, 58, 110–118, <https://doi.org/10.1017/aog.2017.27>, 2017.
- 445 Larsen, S. H., Rutishauser, A., Binder, D., Korsgaard, N., Hynek, B., and Citterio, M.: Glaciological monitoring at A. P. Olsen Ice Cap in NE Greenland, oral, <https://doi.org/10.5194/egusphere-egu23-15647>, 2023.
- Li, X., Sovilla, B., Jiang, C., and Gaume, J.: Three-dimensional and real-scale modeling of flow regimes in dense snow avalanches, *Landslides*, 18, 3393–3406, <https://doi.org/10.1007/s10346-021-01692-8>, 2021.
- 450 Machguth, H., MacFerrin, M., Van As, D., Box, J. E., Charalampidis, C., Colgan, W., Fausto, R. S., Meijer, H. A. J., Mosley-Thompson, E., and Van De Wal, R. S. W.: Greenland meltwater storage in firn limited by near-surface ice formation, *Nature Clim Change*, 6, 390–393, <https://doi.org/10.1038/nclimate2899>, 2016a.
- Machguth, H., Thomsen, H. H., Weidick, A., Ahlstrøm, A. P., Abermann, J., Andersen, M. L., Andersen, S. B., Bjørk, A. A., Box, J. E., Braithwaite, R. J., Bøggild, C. E., Citterio, M., Clement, P., Colgan, W., Fausto, R. S., Gleie, K., Gubler, S., Hasholt, B., Hynek, B., Knudsen, N. T., Larsen, S. H., Mermild, S. H., Oerlemans, J., Oerter, H., Olesen, O. B., Smeets, C. J. P. P., Steffen, K., Stober, M., Sugiyama, S., Van As, D., Van Den Broeke, M. R., and Van De Wal, R. S. W.: Greenland surface mass-balance observations from the ice-sheet ablation area and local glaciers, *Journal of Glaciology*, 62, 861–887, <https://doi.org/10.1017/jog.2016.75>, 2016b.
- 455 Mermild, S. H., Pelto, M., Malmros, J. K., Yde, J. C., Knudsen, N. T., and Hanna, E.: Identification of snow ablation rate, ELA, AAR and net mass balance using transient snowline variations on two Arctic glaciers, *J. Glaciol.*, 59, 649–659, <https://doi.org/10.3189/2013JoG12J221>, 2013.
- 460 Noël, B., Aðalgeirsdóttir, G., Pálsson, F., Wouters, B., Lhermitte, S., Haacker, J. M., and van den Broeke, M. R.: North Atlantic Cooling is Slowing Down Mass Loss of Icelandic Glaciers, *Geophysical Research Letters*, 49, <https://doi.org/10.1029/2021GL095697>, 2022.
- Nuth, C. and Kääb, A.: Co-registration and bias corrections of satellite elevation data sets for quantifying glacier thickness change, *The Cryosphere*, 5, 271–290, <https://doi.org/10.5194/tc-5-271-2011>, 2011.
- Østrem, G. and Brugmann, M.: Glacier Mass Balance Measurements. A manual for field and office work., National Hydrology Research Institute (Canada), 1991.

- Rastner, P., Bolch, T., Mölg, N., Machguth, H., Le Bris, R., and Paul, F.: The first complete inventory of the local glaciers and ice caps on Greenland, *The Cryosphere*, 6, 1483–1495, <https://doi.org/10.5194/tc-6-1483-2012>, 2012.
- 470 Rossini, M., Di Mauro, B., Garzonio, R., Baccolo, G., Cavallini, G., Mattavelli, M., De Amicis, M., and Colombo, R.: Rapid melting dynamics of an alpine glacier with repeated UAV photogrammetry, *Geomorphology*, 304, 159–172, <https://doi.org/10.1016/j.geomorph.2017.12.039>, 2018.
- Schmidt, N. M., Reneerkens, J., Christensen, J. H., Olesen, M., and Roslin, T.: An ecosystem-wide reproductive failure with more snow in the Arctic, *PLoS Biol*, 17, e3000392, <https://doi.org/10.1371/journal.pbio.3000392>, 2019.
- 475 Schöner, W., Binder, D., Hynek, B., Weyss, G., Abermann, J., Olefs, M., and Nicus, U.: Climate change and glacier reaction in Zackenberg Region, National Environmental Research Institute, Aarhus University, Denmark, 2009.
- Sovilla, B., Somavilla, F., and Tomaselli, A.: Measurements of mass balance in dense snow avalanche events, *Ann. Glaciol.*, 32, 230–236, <https://doi.org/10.3189/172756401781819058>, 2001.
- Vandecrux, B., Fausto, R. S., Langen, P. L., Van As, D., MacFerrin, M., Colgan, W. T., Ingeman-Nielsen, T., Steffen, K., Jensen, N. S., Møller, M. T., and Box, J. E.: Drivers of Firn Density on the Greenland Ice Sheet Revealed by Weather Station Observations and Modeling, *JGR Earth Surface*, 123, 2563–2576, <https://doi.org/10.1029/2017JF004597>, 2018.
- World Glacier Monitoring Service (WGMS): Fluctuations of Glaciers Database 2022 (wgms-fog-2022-09), <https://doi.org/10.5904/WGMS-FOG-2022-09>, 2022.
- 485 World Glacier Monitoring Service (WGMS): Fluctuations of Glaciers Database, <https://doi.org/10.5904/WGMS-FOG-2023-09>, 2023.
- Yde, J. C., Gillespie, M. K., Løland, R., Ruud, H., Mernild, S. H., Villiers, S. D., Knudsen, N. T., and Malmros, J. K.: Volume measurements of Mittivakkat Gletscher, southeast Greenland, *J. Glaciol.*, 60, 1199–1207, <https://doi.org/10.3189/2014JoG14J047>, 2014.
- 490 Zemp, M., Thibert, E., Huss, M., Stumm, D., Rolstad Denby, C., Nuth, C., Nussbaumer, S. U., Moholdt, G., Mercer, A., Mayer, C., Joerg, P. C., Jansson, P., Hynek, B., Fischer, A., Escher-Vetter, H., Elvehøy, H., and Andreassen, L. M.: Reanalysing glacier mass balance measurement series, *The Cryosphere*, 7, 1227–1245, <https://doi.org/10.5194/tc-7-1227-2013>, 2013.
- Zemp, M., Huss, M., Thibert, E., Eckert, N., McNabb, R., Huber, J., Barandun, M., Machguth, H., Nussbaumer, S. U., Gärtner-Roer, I., Thomson, L., Paul, F., Maussion, F., Kutuzov, S., and Cogley, J. G.: Global glacier mass changes and their contributions to sea-level rise from 1961 to 2016, *Nature*, 568, 382–386, <https://doi.org/10.1038/s41586-019-1071-0>, 2019.

495



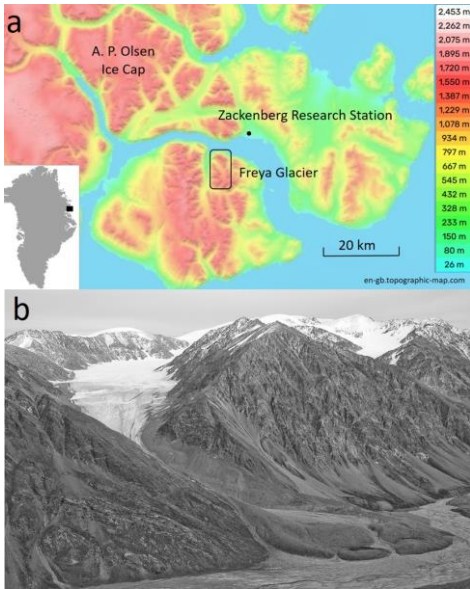


Figure 1: a) Location of Freya (~~Freja~~) Glacier (74.38°N, 20.82°E) on Clavering Island in Northeast Greenland, next to Zackenberg Research Station and A. P. Olsen Ice ~~Cap~~.- (Map from en-gb.topographic-map.com) b) ~~Photo~~-Picture of Freya Glacier and its surrounding ridges in August 2008 (~~Photo~~: B. Hynek).

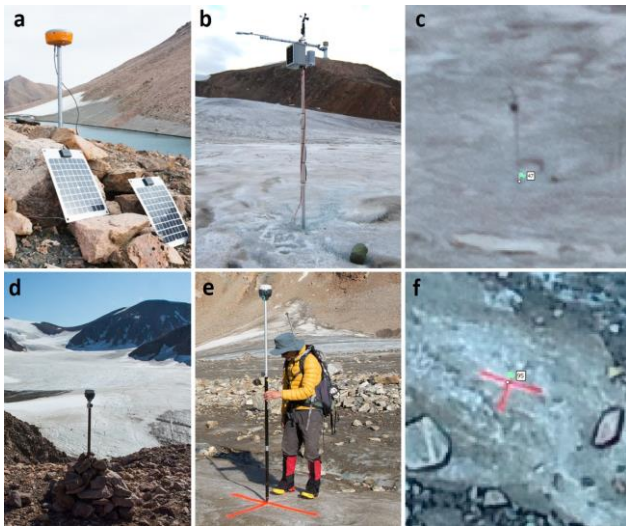
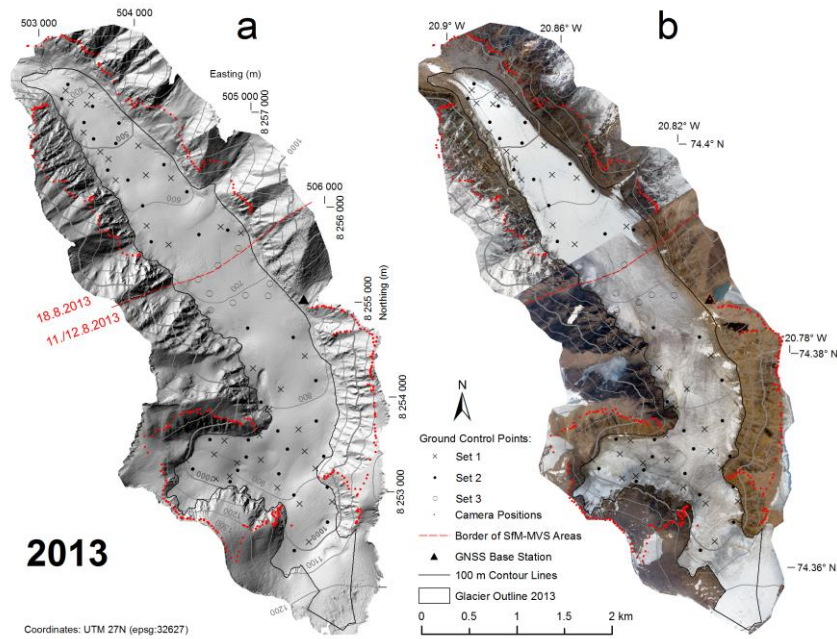


Figure 2: Upper panel: GNSS Survey 2013. a) GNSS base station b) example of a natural GCP and c) its visibility in the imagery. Lower panel: GNSS Survey of 2021. d) GNSS Base Station e) Survey of an artificial GCP and f) ~~its~~-the visibility of the GCP in the imagery.

**Table 1:** Main characteristics of the two SfM-MVS surveys.

	2013	2021
Survey dates	11. - 18.8.2013	27.-31.7.2021
Survey Geometry	Oblique (Terrestrial)	Nadir (UAV)
Camera/UAV	Nikon D7100 + 20mm	Phantom 4 RTK
Image Resolution	24 Mpix	20 Mpix
No of Images	430	6250
Height above glacier surface	10 - 400	140
Ground Sampling Distance	> 20 cm	3.8 cm
No. of visible GCPs	67	68
Density of visible GCPs [ /km <sup>2</sup> ]	12.6	13.6
Max. elevation change during survey [m]	< 0.15	< 0.20
Surface reconstruction [% of Glacier Area]	100%	94%
DEM spatial resolution [m]	1	0.2
Orthophoto spatial resolution [m]	0.25	0.05



**Figure 3:** a) Hillshade of the resulting DEM 2013 in 1m resolution and b) Orthophoto of the survey in August 2013. On both maps the locations of the photo points, the ground control points (GCPs) and the GNSS Base Station are indicated. The upper part of the glacier was surveyed on 11.8. and 12.8. The lower part of the glacier was surveyed on 18.8., after a snow-fall event that marked the end of the ablation season in 2013.

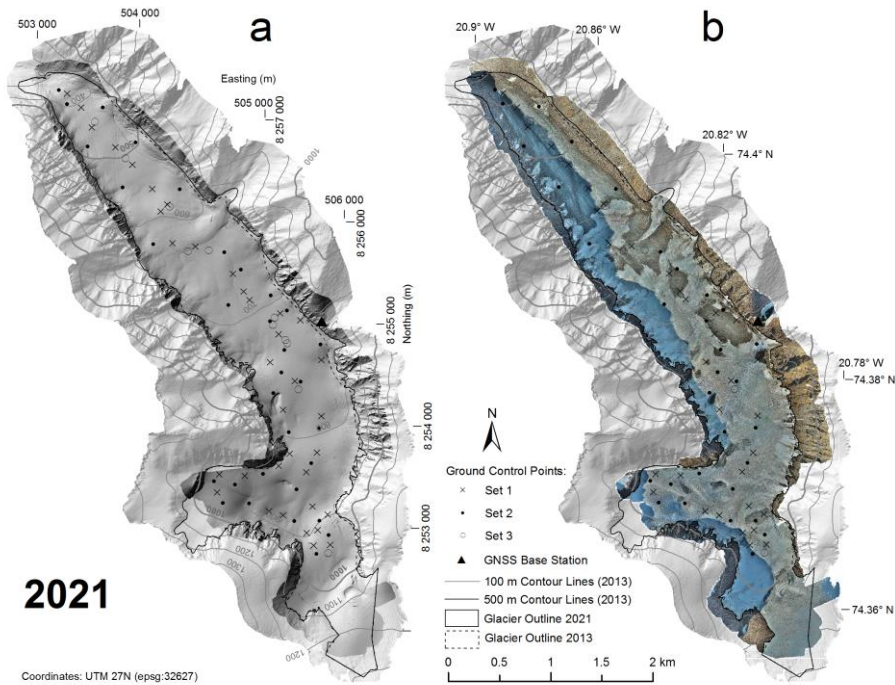


Figure 4: a) Hillshade of the 2021 DEM (dark grey) in 1\_m resolution and b) Orthophoto of the survey in July 2021. On both maps the hillshade of 2013 is displayed in the background and the locations of the ground control points (GCPs) and the ~~GNSS~~-GNSS base station are indicated. The lower part of the glacier was photographed on 27.7.2021 and the upper part on 31.7.2021.

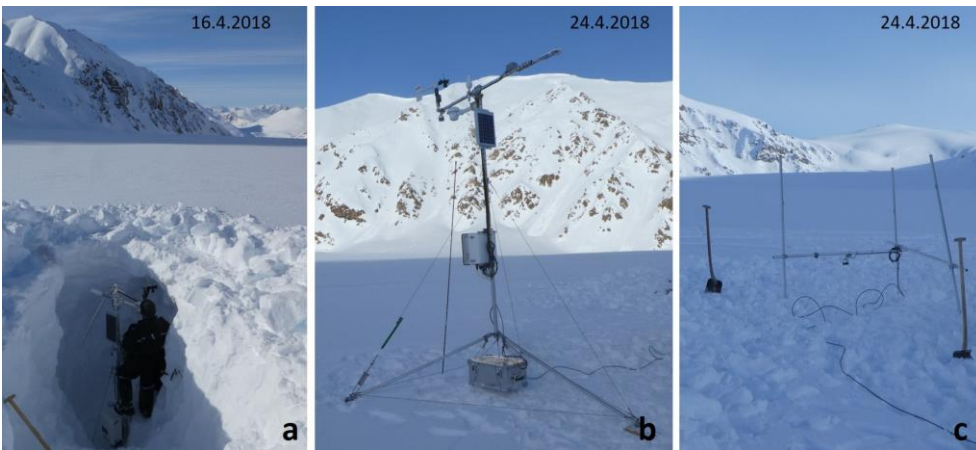


Fig. 5: ~~Maintainenee~~Maintenance of the AWS at Freya Glacier in April 2018: a) The station is 3.5 m tall and was completely covered in snow. b) The weather station and the c) stakes with the second ultrasonic device were ~~reestablished~~re-established on the snow surface. (Photos: Daniel Binder).

Formatiert: Zeilenabstand: Mehrere 1,15 ze

525

530

Table 2: Error statistics of the ground control points in both **sfmSfM**-models

Model	No. of Control Points (Set 2)	RMSE Control Points [m]				No. of Check Points (Set 1)	RMSE Check Points [m]				No. of z-Val Points (Set 3)	RMSE [m]	
		X	Y	Z	TOT		X	Y	Z	TOT		Z	
2013	33	0.14	0.12	0.10	<b>0.21</b>	32	0.41	0.37	0.20	<b>0.59</b>	9	0.37	
2021	31	0.20	0.10	0.16	<b>0.28</b>	36	0.21	0.10	0.18	<b>0.30</b>	11	0.12	

Formatiert: Englisch (Vereinigte Staaten)

Formatiert: Englisch (Vereinigte Staaten)

Formatiert: Englisch (Vereinigte Staaten)

Formatiert: Englisch (Vereinigte Staaten)

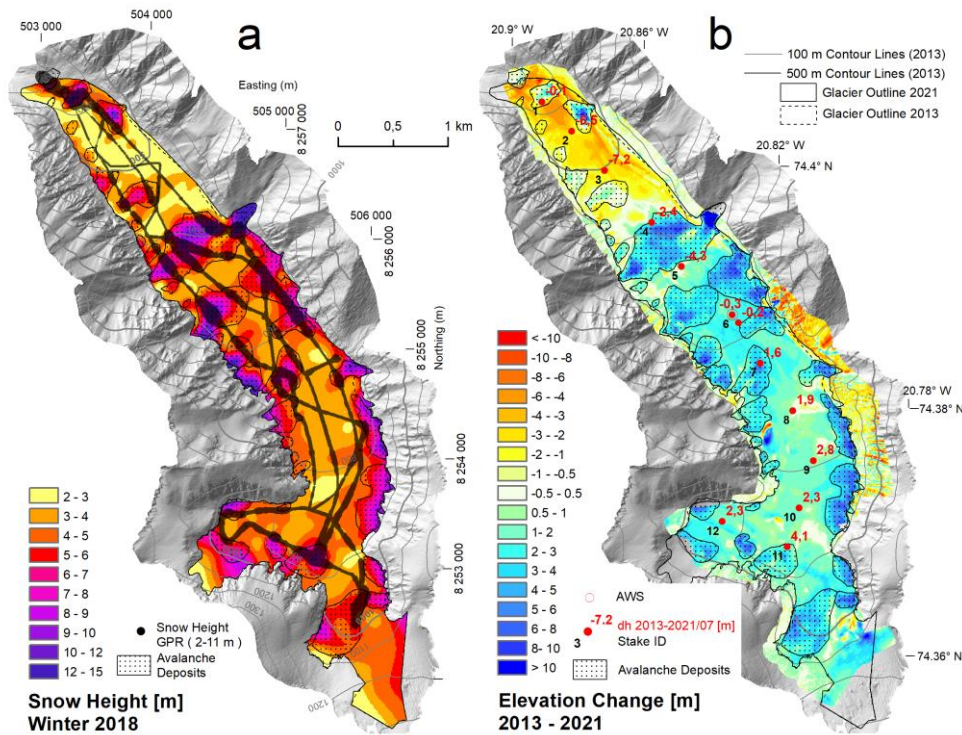


Figure 6: a) Measured (GPR) and extrapolated snow height in winter 2018 and delineation of avalanche affected areas. b) Elevation Change between 18.8.2013 and 27.7.2021. Cumulative measured height changes ablation at the ablation stakes for the same period are shown in red (in m).

535

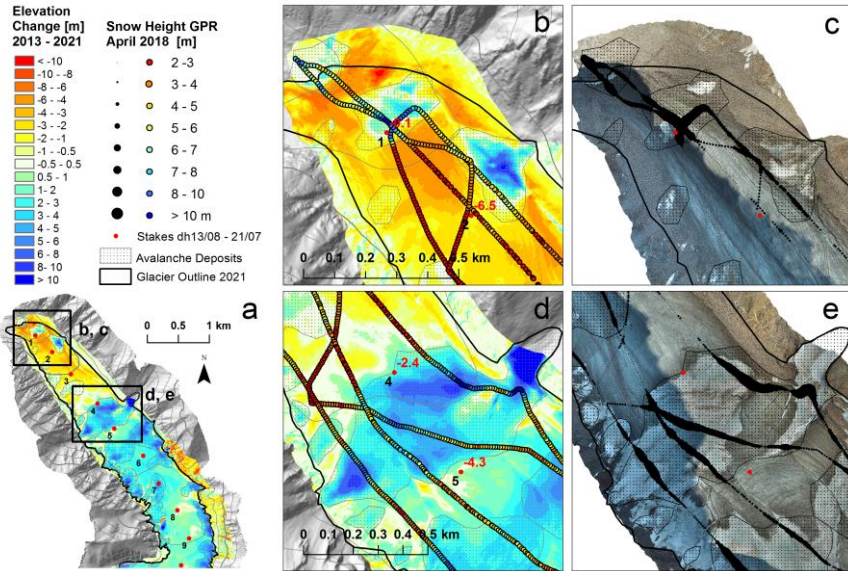


Figure 7: a) Overview and (b, d) close-ups of Elevation Changes and (c, e) Orthophoto 2021 together with GPR snow height data of spring 2018 and measured ablation at the stakes (in m).

540

Table 3: Spatial mean values of the winter balance 2018 and the multi-year geodetic mass balance.

	Spatial Mean on Total Glacier Area	Spatial Mean on Glacier Area affected by avalanches 2018	Spatial Mean on Glacier Area NOT affected by avalanches 2018
Surface Area 2021 [km <sup>2</sup> ]	5.54	1.98	3.55
Surface Area [%]	100%	36%	64%
Elevation change [m] 08/2013 - 07/2021	1.56 +/- 0.15	3.18	0.67
Geodetic mass balance [m w.e.] 08/2013 - 07/2021	1.33 +/- 0.21		
Winter 2018 snow height [m]	4.8	6.2	4.0
Winter mass balance [m w.e.] (same density)	1.85	2.40	1.54
Winter mass balance [m w.e.] (5% density increase)	1.89	2.52	1.54
Winter mass balance [m w.e.] (10% density increase)	1.93	2.64	1.54

545

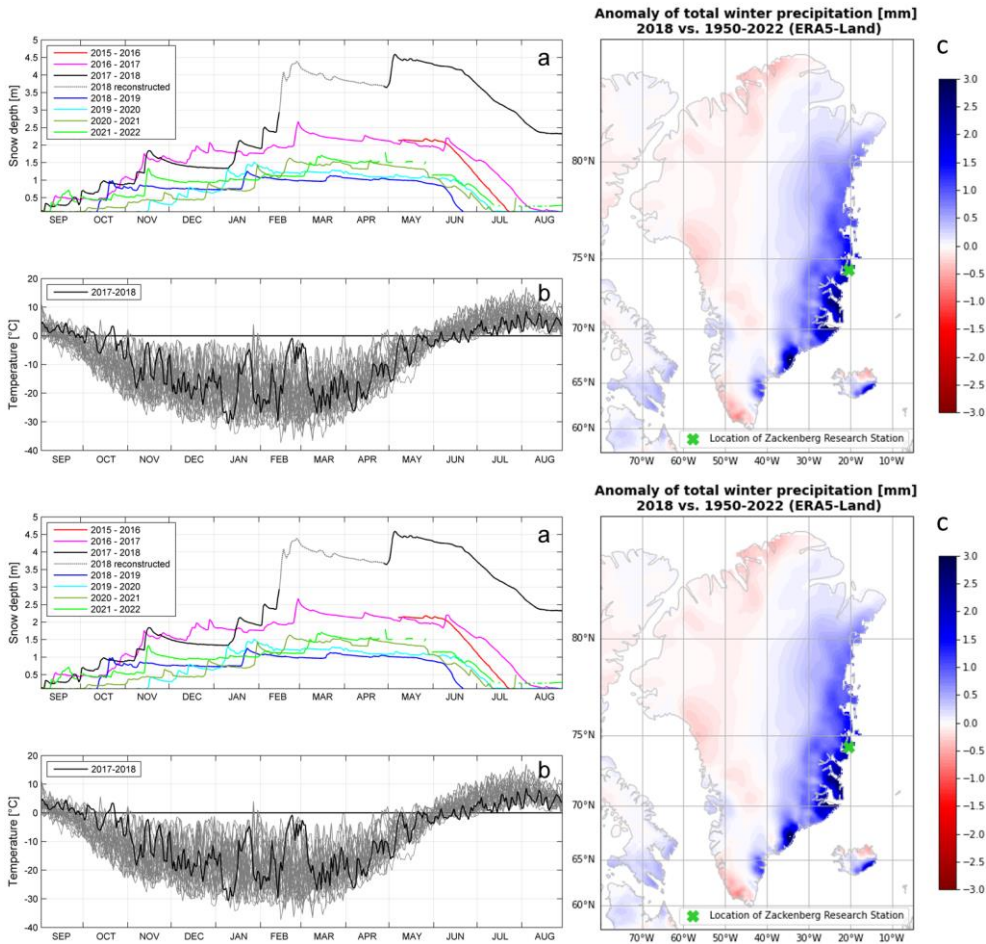


Fig 8: a) Continuous snow depth record from the AWS on Freya Glacier (680 m a.s.l.) since May 2016. b) Daily mean temperature at Zakenberg (37 m a.s.l.) c) Anomaly of ERA 5 cumulative precipitation (SEP-MAY) of 2018.

Formatiert: Zeilenabstand: Mehrere 1,15 ze

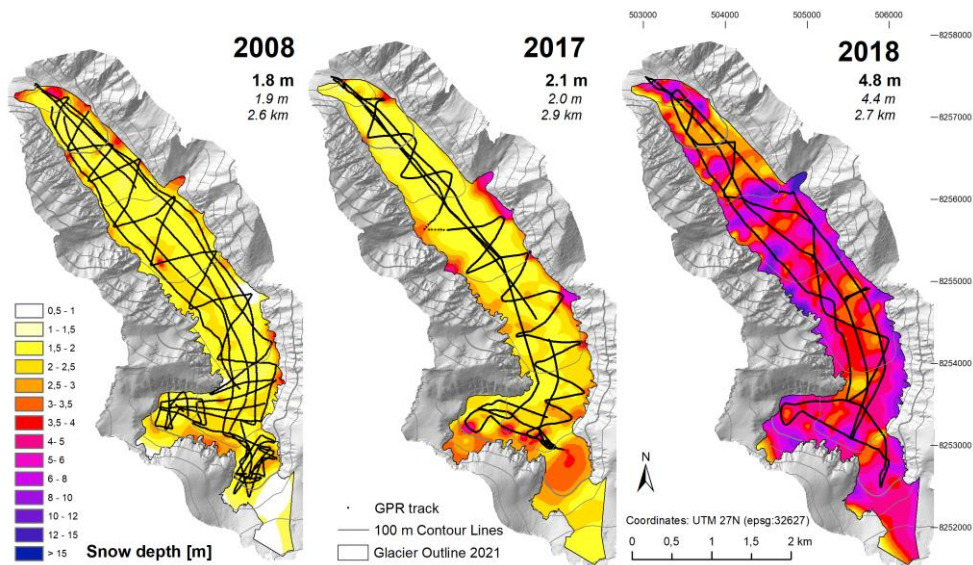


Fig 9: End of winter snow depth maps in years with a detailed GPR survey. Mean ~~snowdepth~~ *snow depth* of the interpolated grid is given in bold, ~~arithmetic~~ *arithmetic* mean of the individual GPR snow depth points is given in italic. Length of the GPR track is given in km.

- Formatiert: Schriftart: 9 Pt.
- Formatiert: Zeilenabstand: Mehrere 1,15 ze
- Formatiert: Schriftart: 9 Pt.
- Formatiert: Schriftart: 9 Pt.

555

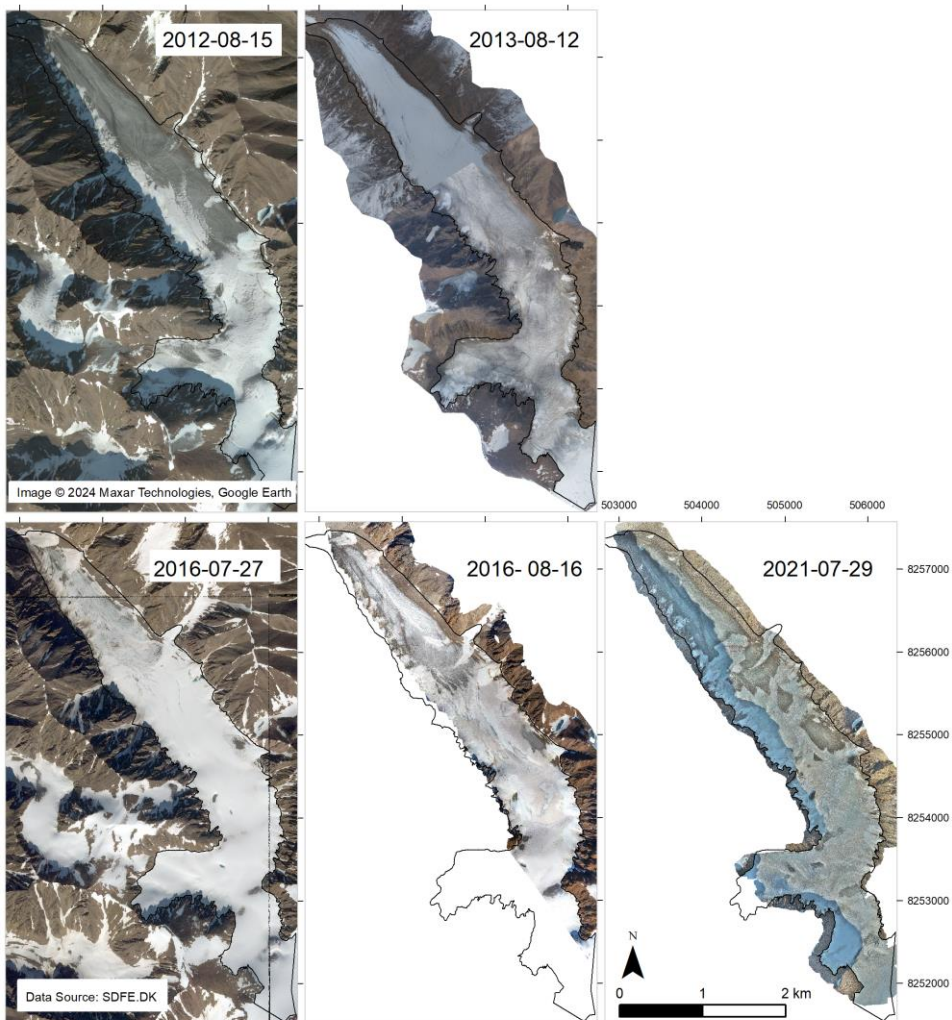


Fig. 10: Orthophotos of Freya Glacier of in 2012, 2013, 2016 and 2021.

Formatiert: Schriftart: 9 Pt.

Formatiert: Schriftart: 9 Pt.

Formatiert: Schriftart: 9 Pt.



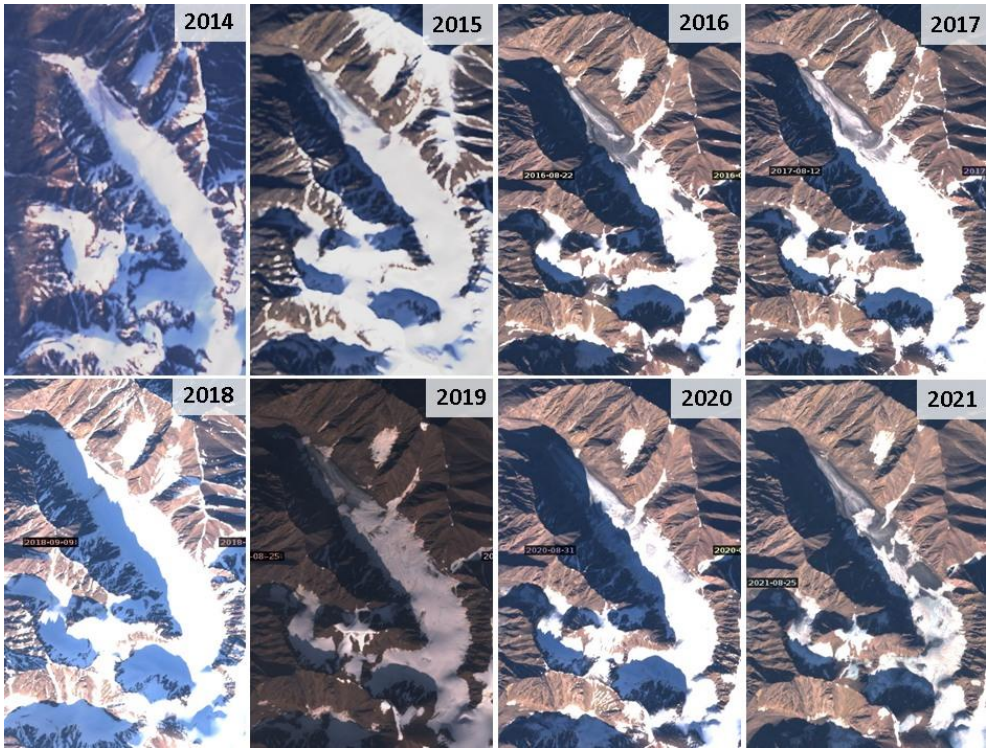


Figure 11: Sentinel 2 (2016-2021) and Landsat (2014-2015) images close to the end of the ablation season show snow cover extent and the remnants of avalanche-affected areas at the end of summer. Landsat images 2014 and 2015 courtesy of the U.S. Geological Survey. Copernicus Sentinel 2 data 2016-2021, processed by ESA were retrieved from Sentinel Hub.

Formatiert: Schriftart: 9 Pt.  
 Formatiert: Zeilenabstand: Mehrere 1,15 ze  
 Formatiert: Schriftart: 9 Pt.

560

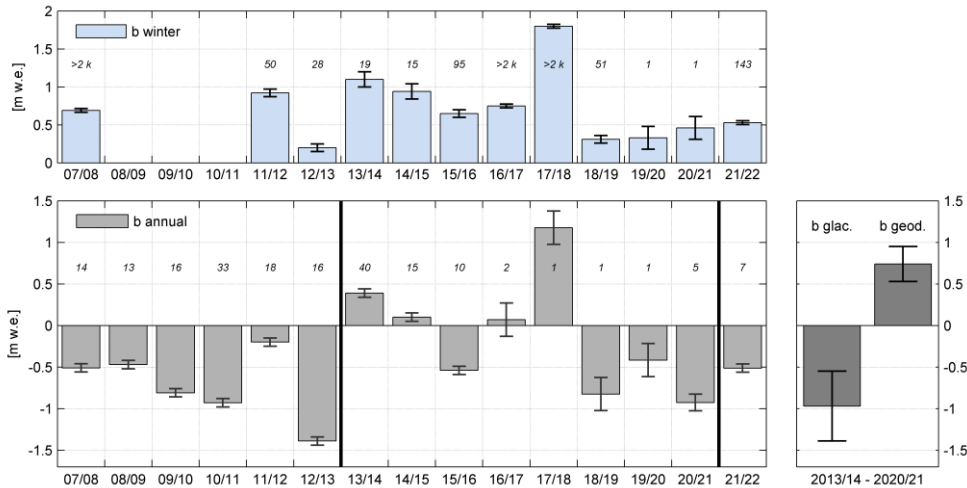


Figure 12: Left panels: Time series of specific winter mass balances (top), and specific annual mass balances (bottom) with their estimated uncertainties. The number of point observations available for the mass balance calculation of individual years (winters) is shown as italic numbers. E.g. winter mass balance 2017/18 is based on more than 2000 point observations, while annual balance 2017/18 is based on one point observation only. Right panel: Comparison of the cumulative glaciological and geodetic mass balance 2013/14 – 2020/21 and their related uncertainties.

<sup>1</sup> According to the Language Secretariat of Greenland (Oqasileriffik.gl) the official name is spelled as *Frejagletsjer* (formerly *Frejagletcher*). While (Ahlmann, 1946) used *Frøya Glacier*, in (Higgins, 2010) the glacier was also spelled as *Fröjabreen*, *Frøya Glacier* and *Frøya Glacier*. In recent scientific literature (e.g. Schönner et al., 2009) the spelling *Freya Glacier* has been used.

- Formatiert: Schriftart: Kursiv
- Formatiert: Schriftart: Kursiv
- Formatiert: Schriftart: Kursiv
- Formatiert: Schriftart: Kursiv
- Formatiert: Schriftart: Kursiv
- Formatiert: Schriftart: Kursiv